

## Compatibilizing effects of block copolymers in low-density polyethylene/polystyrene blends

H. F. Guo, S. Packirisamy†, R. S. Mani††, C. L. Aronson‡, N. V. Gvozdic and D. J. Meier\*

Michigan Molecular Institute, 1910 West St. Andrews Road, Midland, MI 48640-2696, USA

(Received 17 June 1996; revised 23 May 1997; accepted 10 July 1997)

The phase and mechanical properties of a low-density polyethylene/polystyrene 70/30 (LDPE/PS 70/30) blend has been determined after compatibilization with various styrene–ethylene, styrene–ethylene/butene and styrene–ethylene/propylene type block copolymers. It is shown that high interfacial activity, as reflected in the reduction of the dispersed phase size, does not necessarily bring about an improvement in the mechanical properties of the blend. Although the diblock copolymers were more efficient in reducing the phase size, the triblock copolymers were more effective in improving the mechanical properties. The effect of a poly(styrene-*b*-ethylene) (S–E) block copolymer on the particle coalescence and rheological properties of the LDPE/PS 70/30 blend has been investigated. It is shown that small amounts of the block copolymer can significantly retard or actually suppress the coalescence of the dispersed phases, and thus stabilize the morphology of the blend. The addition of the S–E copolymer increases the elastic modulus and dynamic viscosity of the blend, and the samples become more non-Newtonian as the block copolymer concentration increases. © 1998 Published by Elsevier Science Ltd. All rights reserved.

(Keywords: blend; compatibilization; morphology)

### INTRODUCTION

Simple blends of immiscible polymers usually have large dispersed phases and weak interphase adhesion, with resulting poor mechanical properties. Therefore, modification of polymer blends by ‘compatibilization’ with interfacially active compatibilizers (usually block or graft copolymers) has been widely investigated and applied in practice. An effective compatibilizer modifies the phase morphology and the interfacial adhesion of a blend by: (1) reducing the interfacial tension between the two phases and hence leading to a finer dispersion of one phase in another, (2) enhancing adhesion by coupling the phases together and (3) stabilizing the dispersed phase against coalescence<sup>1,2</sup>.

Various techniques can be used to evaluate the effectiveness of a compatibilizer and compatibilization process. Locke and Paul<sup>3</sup>, Heikens *et al.*<sup>4</sup>, and Fayt *et al.*<sup>5–10</sup> reported the beneficial effects on the mechanical properties of PE/PS blends which were compatibilized with different block or graft copolymers. The improvements were attributed to the stronger interfacial adhesion and the smaller particle size of the dispersed phase. With a TEM, Teyssie and co-workers<sup>9</sup> clearly demonstrated that a poly(styrene-*b*-ethylene) (S–E) block copolymer locates at the interface by showing that the block copolymer formed a continuous layer around the dispersed phase. The interfacial activity of copolymers has also been characterized by interfacial tension measurements<sup>11–16</sup>. Most studies found that interfacial

tension decreased exponentially with the amount of the compatibilizer used, with a sharp decrease at the beginning followed by a leveling off at higher concentrations.

It is recognized that the molecular architecture of a compatibilizer is critical to its interfacial efficiency. Theories<sup>17–20</sup> suggest that the most desirable compatibilizer from the standpoint of the reduction of interfacial tension in a system of polymers A and B is a symmetric diblock copolymer A–B. Since the interfacial activity increases with increasing chain length, the block chain lengths must be relatively long, but an upper limit exists due to micelle formation. Many experimental studies<sup>5,7,21–25</sup> have arrived at similar conclusions. However, detailed and systematic investigations of the interplay between the interfacial activity and the ability of the block copolymer to improve mechanical properties of compatibilized polymer blends are still lacking, especially in mechanically mixed systems. In this work, several di- and triblock copolymers having various compositions and structures were used to compatibilize a binary blend of LDPE and PS. Their effects on the morphological and mechanical properties of the blend were investigated. The relationship, if any, between the interfacial activity (as judged by phase size) and the ability to improve mechanical properties of these block copolymers was particularly of concern.

Small particles of the dispersed polymer phase in a molten blend tend to coalesce into larger ones, driven by the tendency for the system to minimize the interfacial free energy. The rate of coalescence is highly dependent on the concentration of the minor phase and the viscosity of the matrix<sup>26–30</sup>. Since manufactured polymer products are often annealed and coalescence may occur during annealing with a change in properties, the control of the particle coalescence is very important. Studies have shown that copolymers can stabilize morphologies of blends against

\* To whom correspondence should be addressed

† Present address: Vikram Sarabhai Space Center, Indian Space Research Organization, Trivandrum 695022, India

†† Present address: Optical Polymer Research Inc., Gainesville, FL 32609, USA

‡ Present address: Macromolecular Science and Engineering Center, The University of Michigan, Ann Arbor, MI 48109, USA

particle coalescence<sup>26,31-34</sup>. Theoretical work<sup>17</sup> suggests that about 2% of a typical diblock copolymer can completely cover 1- $\mu\text{m}$ -size particles of the dispersed phases and much less might be needed just to stabilize the morphology<sup>18,35</sup>. However, experimental data are lacking to show what amount of an efficient block copolymer is required to retard coalescence. In this paper, the effect of added poly(styrene-*b*-ethylene) block copolymer on the kinetics of particle coalescence of a LDPE/PS 70/30 blend is quantitatively assessed.

The rheological properties of polymer blends compatibilized with block copolymers are also discussed. The flow properties of polymer blends depend, among other factors, on the morphology and on the interfacial properties. A modification of the morphology by added compatibilizers, e.g., reduction in particle size or interfacial tension, can result in a change in the flow properties. Since the rheological behavior of immiscible polymer blends is generally very complex, the effect of copolymers on rheological properties of such blends remains controversial. Utracki and Sammut<sup>36</sup> studied the effect of poly(styrene-*b*-butadiene-*b*-styrene) (S-B-S) block copolymer on rheological properties of PE/PS blends under steady-shear flow. No significant effect of this copolymer was found on either the morphological or rheological properties of the blend, presumably because an S-B-S block copolymer is not expected to be particularly interfacially active in a PE/PS blend. On the other hand, Haaga and Friedrich<sup>37</sup> reported that addition of a poly(styrene-*b*-ethylene/butene-*b*-styrene) (S-EB-S) block copolymer increased the dynamic viscosity of PE/PS blends. They and Riemann *et al.*<sup>38</sup> reported that the blends with block copolymers showed additional elastic effects in the low frequency range compared to the blends without block copolymers, while Bousmina *et al.*<sup>39</sup> came to the opposite conclusion for such PS/PE blends with S-EB-S block copolymers. Kim and Meier<sup>40</sup> showed that the shear viscosity of PE/PS blends was increased by additions of different poly(styrene-*b*-ethylene) (S-E) diblock and poly(styrene-*b*-ethylene-*b*-styrene) (S-E-S) triblock copolymers. Brahim *et al.*<sup>41</sup> reported that the effect of block copolymer was very sensitive to the concentration of the block copolymer. They found that the addition of 1% of a tapered poly(styrene-*b*-hydrogenated butadiene) diblock copolymer decreased the viscosity and elastic modulus of a high-density polyethylene/high-impact polystyrene (HDPE/HIPS) blend, while the opposite behavior was observed when the blend contained 5% copolymer. They interpreted this behavior as due to the change in the state of the copolymer in the blend, i.e., saturation of the interface and micelle formation. In this paper, the effects of a poly(styrene-*b*-ethylene) block copolymer on the rheological properties of LDPE/PS blends, which are qualitatively correlated with the morphologies of the blend and with the block copolymer concentration, will be reported.

## EXPERIMENTAL

### Materials

The homopolymers used in this study were commercial products. Polystyrene (PS) was Styron<sup>®</sup> 666D from Dow Chemical Company, with molecular weight  $M_w = 260\,000$  and  $M_n = 160\,000$ . Low-density polyethylene (LDPE) was obtained from Eastman Organic Chemicals with molecular weight  $M_n = 13\,500$  (Catalog No. 6018).

The poly(styrene-*b*-ethylene) (S-E) block copolymer was prepared in this work by the sequential anionic

polymerization of a poly(styrene-*b*-butadiene) (S-B) block copolymer on a vacuum line and the subsequent hydrogenation of the butadiene component. The poly(styrene-*b*-ethylene-*b*-styrene) (S-E-S) triblock copolymer was prepared by the hydrogenation of the butadiene block of a poly(styrene-*b*-butadiene-*b*-styrene) (S-B-S) block copolymer. The poly(styrene-*b*-ethylene/butene-*b*-styrene) (S-EB-S) and poly(styrene-*b*-ethylene/propylene) (S-EP) block copolymers were gifts from the Shell Chemical Co., with code names of TRW-7-1051 and TRW-7-1049, respectively. The properties of these copolymers are given in Table 1.

### Poly(styrene-*b*-ethylene) synthesis

A poly(styrene-*b*-butadiene) (S-B) block copolymer was prepared by first polymerizing the butadiene block. The desired amount of *n*-butyl lithium initiator was added through a septum into a polymerization flask containing a solution of butadiene in cyclohexane at  $-78^\circ\text{C}$ . The reaction mixture was slowly warmed to  $60^\circ\text{C}$  and maintained at this temperature under  $\text{N}_2$  for 3 h, at which time the solution was very viscous. Then purified styrene monomer was added from an attached measuring cylinder into the polybutadiene solution, which then became red-orange in color. The polymerization of styrene was done at  $60^\circ\text{C}$  for 30 min. After cooling the reaction mixture to  $25^\circ\text{C}$ , the pressure inside the flask was released and the polymer was precipitated in an excess volume of methanol. The block copolymer was filtered and dried under vacuum at  $70^\circ\text{C}$  for 16 h. The mole ratio of 1,4- and 1,2-microstructure of the polybutadiene was determined by  $^1\text{H}$  n.m.r. analysis to be 94:6. The composition of the copolymer was also determined by the  $^1\text{H}$  n.m.r. analysis, while the molecular weight was obtained by gel permeation chromatography (GPC).

The poly(styrene-*b*-ethylene) (S-E) block copolymer was obtained from poly(styrene-*b*-butadiene) by hydrogenation of the butadiene block. S-B was dissolved in 500 ml of *o*-xylene in a 2-l flask. To this solution two equivalents of *p*-toluene sulfonyl hydrazide and two equivalents of *n*-tripropylamine were added and the solution was heated to the reflux temperature of *o*-xylene and maintained at this temperature for 12 h. The solution was cooled to  $25^\circ\text{C}$  and washed twice with 500 ml of distilled water. The organic layer was separated and passed through activated aluminum to remove any water, and then poured into an excess volume of methanol. The precipitated polymer was filtered and dried under vacuum at  $70^\circ\text{C}$  for 16 h.  $^1\text{H}$  n.m.r. analysis confirmed that the butadiene block was completely hydrogenated.

### Blend preparations and characterizations

All the blends were prepared on a Haake Rheocord<sup>®</sup> 90 torque rheometer by adding the dry-mixed blend components to a 60-ml batch mixer equipped with a pair of roller blades, and mixing at  $200^\circ\text{C}$  and 100 r.p.m. for 10 min. The weight percentage of the block copolymer in each blend is based on the final weight of the blend.

After blending, the samples were compression molded into sheets or into tensile test specimens with a Pasadena hydraulic press at  $200^\circ\text{C}$ , 300 p.s.i. for 5 min. The compression molded sheets of the blends were fractured in liquid nitrogen, and the resulting fracture surfaces were coated with gold and carbon. An AMRAY 1820 scanning electron microscope (SEM) was used to study morphologies of these samples. Tensile tests were done at room

temperature using dumbbell-shaped specimens and with an Instron Universal Testing Instrument, following ASTM D1708 testing specifications. Each reported value is the average of at least five tests.

#### Coalescence studies

For coalescence study, blend samples were annealed at 200°C with a Pasadena hydraulic press at 300 p.s.i. for different lengths of annealing time. Since it took about 1–2 min for the sample to be taken out of the mixer and to be cooled down to below the  $T_g$  of PS after annealing, the real coalescence time was 1–2 min longer than the reported annealing time. The annealed sample sheets were then fractured in liquid nitrogen and the resulting fracture surfaces etched with cyclohexane to remove the PS particles. SEM was used to study these samples, and the volume-average diameters of the dispersed phases were determined from the micrographs.

#### Rheological measurements

The dynamic rheological properties were measured on a Rheometrics RMS-605 Mechanical Spectrometer using parallel-plate geometry with 25-mm diameter platens and a gap of ~1 mm. Test samples of 25 mm diameter were cut from the compression-molded sheets after they had been annealed at 200°C for 5 min. Frequency sweeps from 0.025 to 100 rad/s were carried out at a temperature of 180°C and at a strain level of 15%. The experiments were performed under a continuous purge of dry nitrogen, and repeated measurements showed that thermal degradation was not a problem.

## RESULTS AND DISCUSSION

#### Morphologies and mechanical properties

Four block copolymers having different structures and compositions (Table 1) were used to evaluate their effectiveness in compatibilizing blends of LDPE/PS (70/30). These included a S–E diblock and a S–E–S triblock, each having almost the same overall molecular weight and composition. Also included were S–EB–S triblock and S–EP diblock copolymers, which differed not only in composition but also in structure (the EB–block in S–EB–S is a random ethylene/butene block, and the EP–block in S–EP is an alternating ethylene/propylene block). In contrast to the S–E and S–E–S copolymers which have a crystallizable ethylene block (E–block), the EB–block of S–EB–S and the EP–block of S–EP are non-crystalline.

Figure 1A shows an SEM micrograph of the fracture surface of LDPE/PS (70/30). The dispersed PS particles have a broad size distribution and a smooth surface. Figure 1B–E shows the fracture surfaces of the blends to which 1% of different block copolymers have been added. Significant decreases in particle sizes are shown for all the blends which contain block copolymers, especially so for the sample containing the S–E block copolymer shown in

Figure 1B (note the difference in magnification of this photo with the others). In addition, the PS particles show fracture surfaces, indicating better interfacial adhesion of the PS particles to the LDPE matrix. Etching of the fracture surfaces with cyclohexane to remove the polystyrene particles improved the accuracy of determining the PS phase sizes by SEM. Figure 2 shows the volume-average diameter  $d_v$  of the PS phase size for the different block copolymers. The  $d_v$  decreased from 6.6  $\mu\text{m}$  for the uncompatibilized sample to 0.9  $\mu\text{m}$  for the sample containing S–E, and to 1.5  $\mu\text{m}$  for the sample with S–E–S. The S–EP and S–EB–S block copolymers are also interfacially active, reducing the  $d_v$  of the blends to 2.0 and 2.8  $\mu\text{m}$ , respectively.

The tensile properties of these blends are shown in Figure 3A and Figure 3B. Here the S–E–S triblock copolymer clearly improves the mechanical properties of the blend to a greater degree than does the S–E diblock copolymer, in spite of the better interfacial activity of the S–E diblock (as judged from the dispersed phase size shown in Figure 2). We believe that this results from the ability of the three blocks of the S–E–S block copolymer to form stronger entanglements (e.g., ‘hairpin loops’) in the interface region.

Comparing the S–EB–S and S–EP block copolymers, the S–EB–S very effectively improves both the tensile strength and the elongation at break of the blend, while the S–EP shows very little effect, even though the S–EP is more effective in reducing the phase size, as shown in Figure 2. Again, the possible formations of entanglements by the triblock S–EB–S in the interfacial region may contribute to its greater effectiveness in improving the mechanical properties of the blend. However, another possibility could be from co-crystallization of the ethylene part in the EB block of S–EB–S with the polyethylene matrix to give good interfacial bounding, as discussed by Kim and Meier<sup>23</sup>. Such co-crystallization is not possible for the alternating EP block of S–EP. Our results clearly indicate that a compatibilizer which is most efficient in reducing the phase size of a blend does not guarantee that it will be the most efficient in improving the mechanical properties of the blend.

#### Effects of the block copolymer concentration

The dependence of the volume-average diameter  $d_v$  of the PS particles on the S–E copolymer concentration for LDPE/PS (70/30) blends is shown in Figure 4. A continuous decrease in  $d_v$  is observed and eventually a quasi-equilibrium particle size can be attained. This quasi-equilibrium particle size is believed to be mainly the result of kinetic factors, i.e., the balance between shear forces which tend to disrupt a particle and the interfacial tension forces which tend to resist deformation and disintegration, as explained by Taylor theory of droplet breakup<sup>42,43</sup>. The theory predicts a decrease in the dispersed phase size with a lowering of interfacial tension and the subsequent attainment of a limiting diameter due to the balance between the interfacial and the shear forces.

Assuming that all the S–E goes to the interface, it is possible to calculate the surface coverage  $\Sigma$ , defined as the number of copolymer chains per unit area of the interface, by using the following equation<sup>1</sup>:

$$\Sigma = RN\phi_{BCP}/3\phi_A M$$

where  $\phi_A$  is the volume fraction of the dispersed phase in the form of spherical particles of radius  $R$ ,  $M$  is the

**Table 1** Characteristics of poly(styrene-*b*-ethylene) and other block copolymers

Reference	Composition	Molecular weight	Code name
S–E diblock	50 wt% PS	36.5–36.5k	SE-1
S–E–S triblock	59 wt% PS	20–31–24k	SES-1
S–EB–S triblock	29 wt% PS	10–50–10k	Shell TRW-7-1051
S–EP diblock	36 wt% PS	36–65k	Shell TRW-7-1049

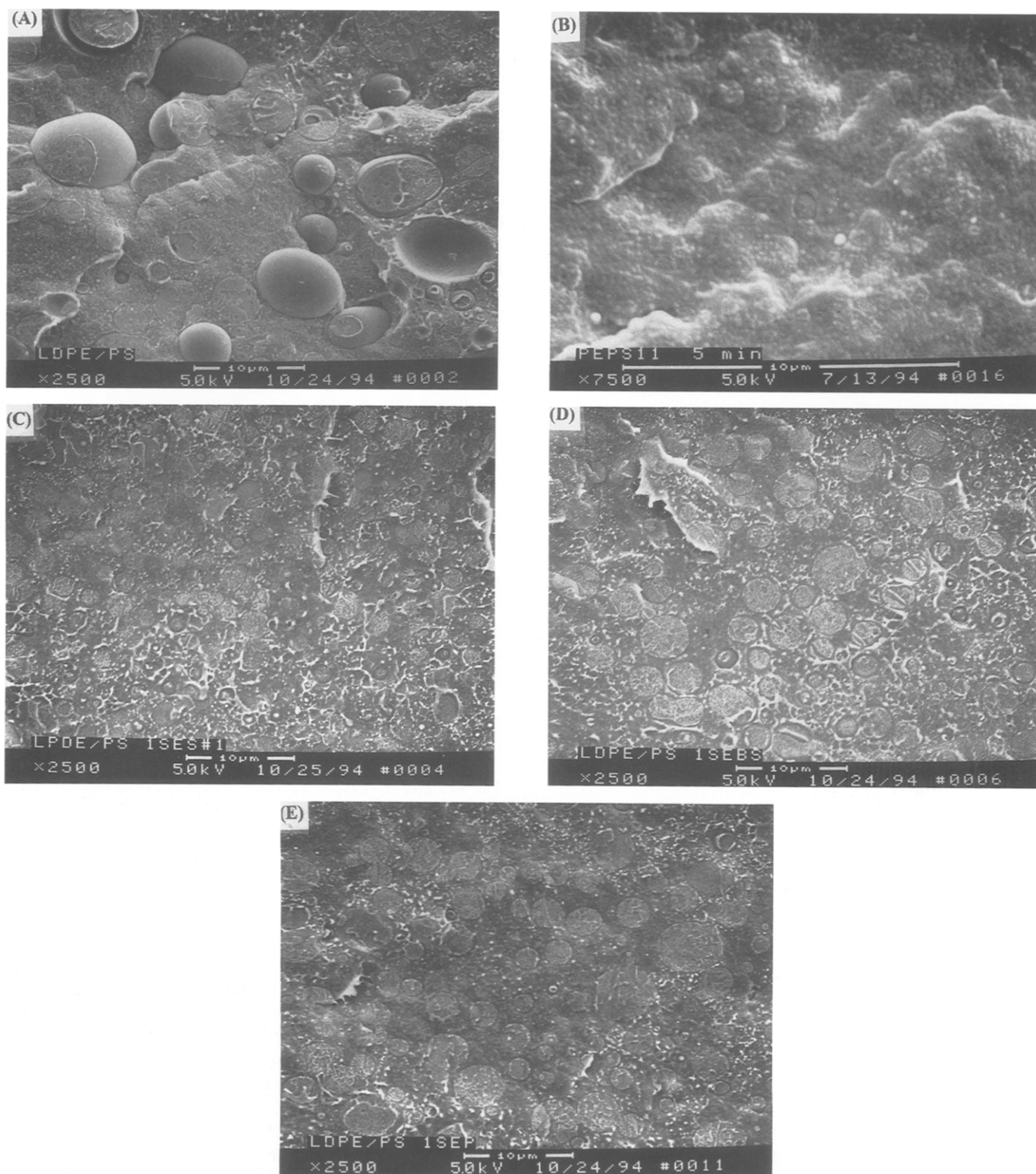


**Figure 1** SEM micrographs of the fracture surfaces of LDPE/PS (70/30) blends compatibilized with: (A) 0% block copolymer; (B) 1% S-E; (C) 1% S-E-S; (D) 1% S-EB-S; and (E) 1% S-EP block copolymers. Note the higher magnification in (B)

molecular weight of the copolymer,  $\phi_{BCP}$  is the volume fraction of the copolymer in the blend, and  $N$  is Avogadro's number. Calculated surface coverages (Table 2) for our LDPE/PS blends are 0.023, 0.037 and 0.064 chains/nm<sup>2</sup> for S-E concentrations of 0.25, 1 and 3%, respectively.

#### Particle coalescence

The influence of the S-E copolymer on the particle coalescence behavior of the LDPE/PS 70/30 blend was investigated. Figure 5 shows SEM micrographs of the fracture surfaces of the uncompatibilized blend annealed at

200°C for 0 and 5 min. The pictures clearly show that the PS particles grew significantly during the 5 min of annealing, with the volume-average diameter ( $d_v$ ) increasing from 5.5 to 7.3 µm. Although Jang *et al.*<sup>28</sup> reported that a broader phase size distribution resulted from the annealing of polypropylene/ethylene-propylene-diene rubber blends, we did not find any obvious change in the phase size distribution after annealing, as Figure 6 shows. Favis<sup>29</sup> also reported that no change in size distribution for polypropylene/polycarbonate blends was found.

The growth of the dispersed particles results from two

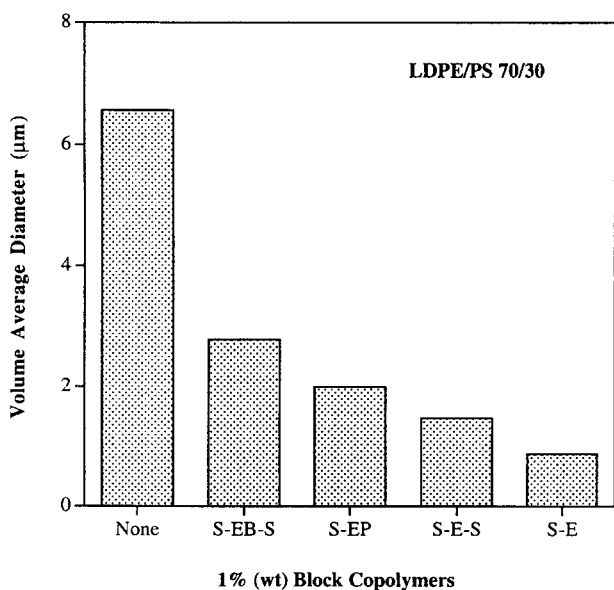


**Figure 2** Volume-average PS phase diameter in LDPE/PS (70/30) blends versus different block copolymers of different structures

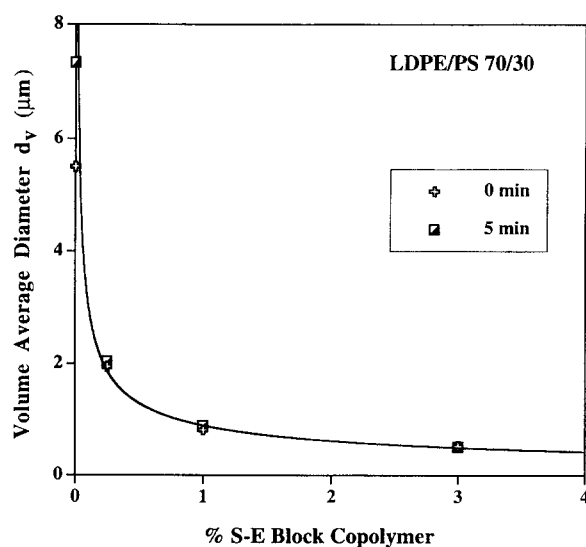


**Figure 4** Volume-average diameter  $d_v$  of LDPE/PS 70/30 blends versus the concentration of the S-E block copolymer

**Table 2** Surface coverages of PS particles by S-E

% (w/w) of S-E	$\Sigma$ (chains/nm <sup>2</sup> )
0.25	0.023
1	0.037
3	0.064

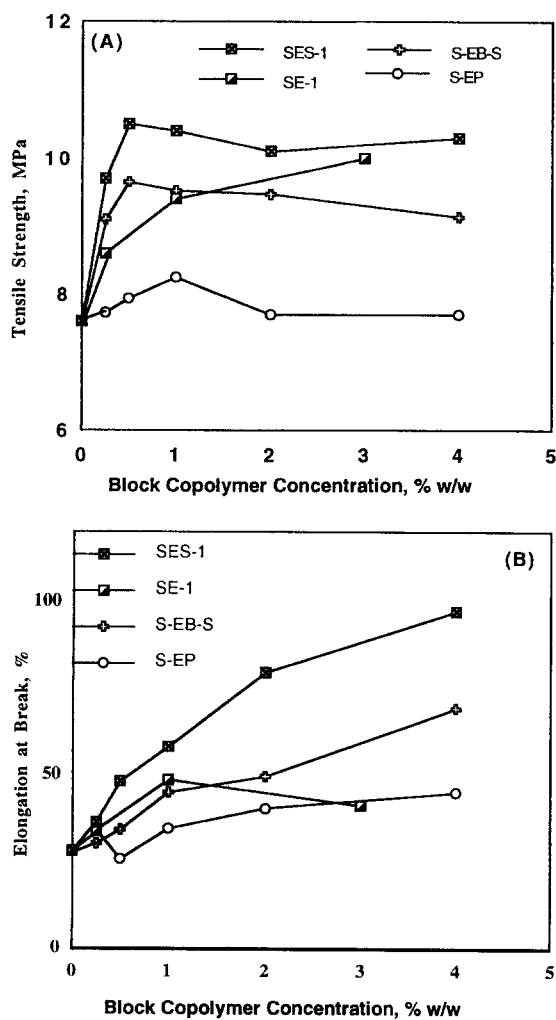


**Figure 3** Tensile properties of LDPE/PS (70/30) blends compatibilized with different block copolymers: (A) tensile strength; (B) elongation at break

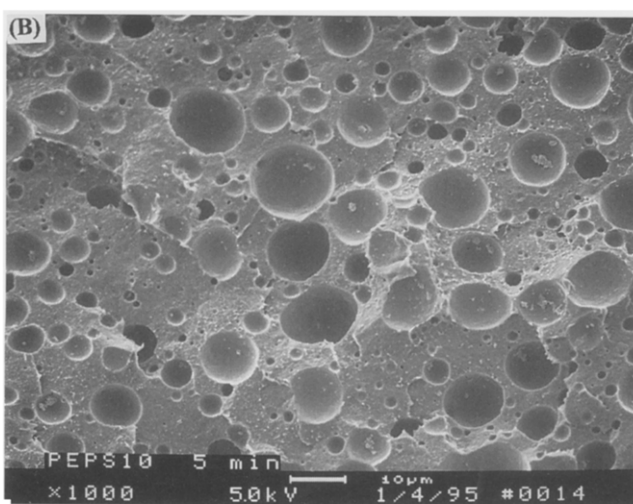
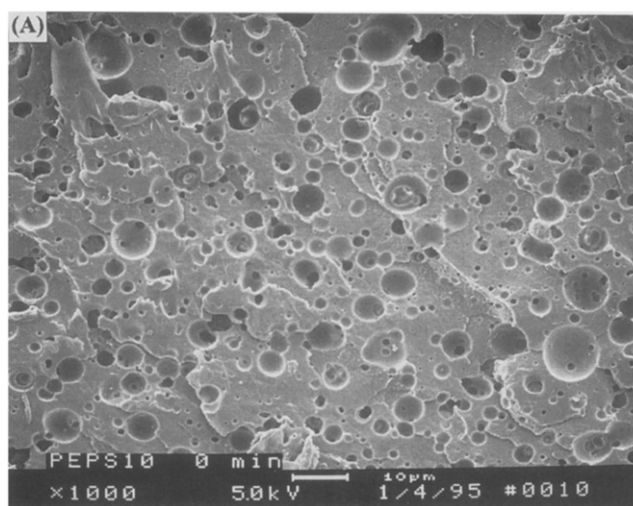


**Figure 5** SEM micrographs of fracture surfaces of LDPE/PS 70/30 blend: (A) before annealing; (B) after 5 min of annealing at 200°C

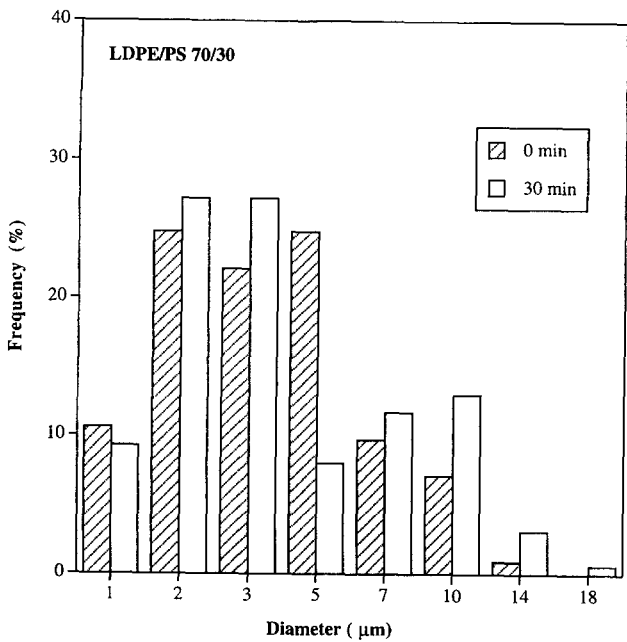


Figure 6 PS phase size distribution before and after 30 min of annealing at 200°C for a LDPE/PS 70/30 blend

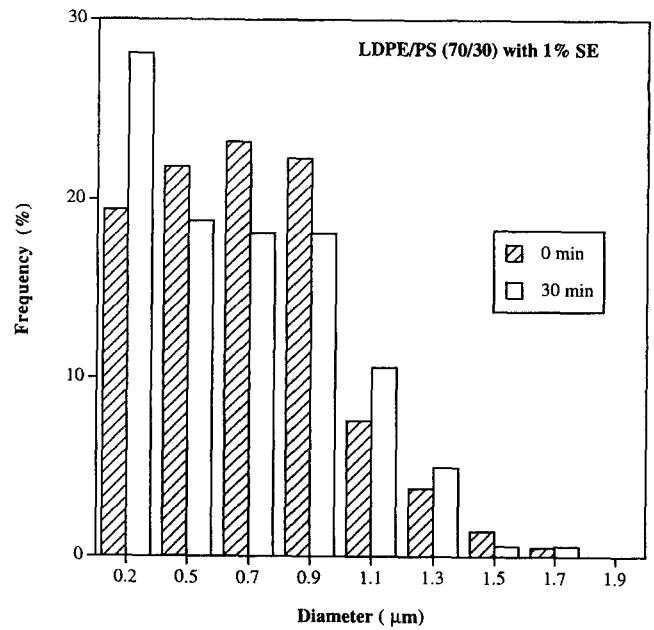


Figure 8 PS phase size distribution before and after 30 min of annealing at 200°C for a LDPE/PS 70/30 blend containing 1% S-E

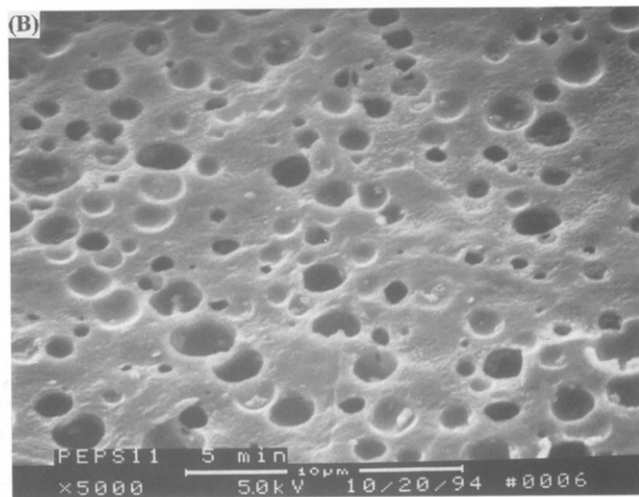
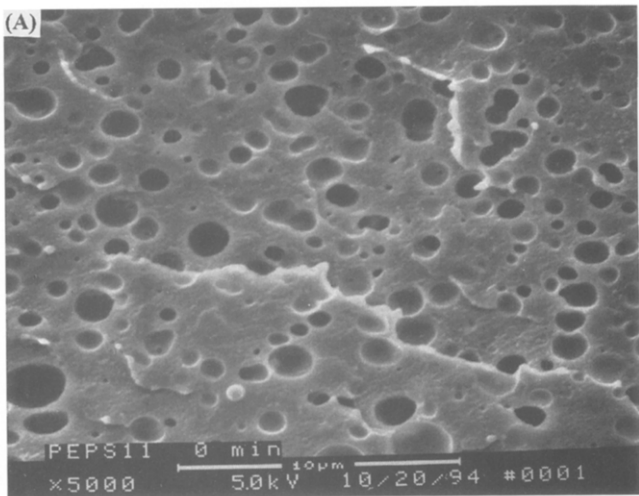


Figure 7 SEM micrographs of fracture surfaces of a LDPE/PS 70/30 blend containing 1% S-E: (A) before annealing; (B) after 5 min of annealing at 200°C

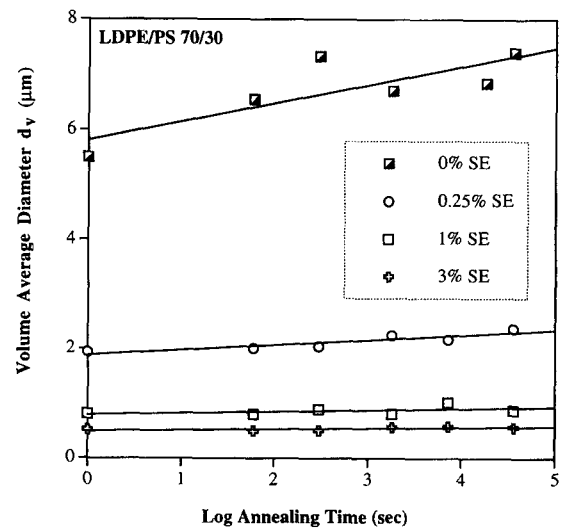
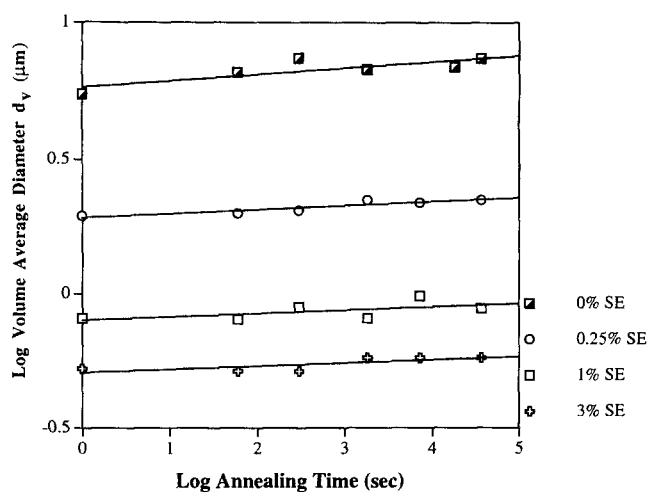
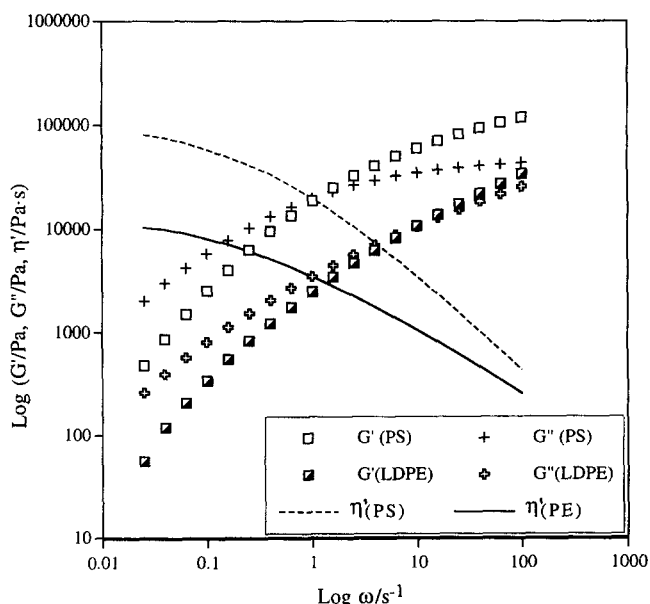


Figure 9 Volume-average diameter  $d_v$  of LDPE/PS 70/30 blends containing different amounts of S-E as the function of the log annealing time

processes: particle contact followed by coalescence to minimize the interfacial energy through minimization of their interfacial area. The interfacial tension is thus the driving 'force' for coalescence. However, the kinetics of the process leading to particle contact remain a puzzle. The diffusional transport of particles, either by random Brownian motion or by Van der Waals attraction, appears to be much too slow to account for the rate of particle growth observed here. An alternative mechanism for particle growth could be the dissolution of polymer molecules from the particles and their diffusional transport from one particle to another (particularly the transport from the smaller to the larger particles because of the enhanced chemical potential of molecules in the smaller particles). The diffusional transport rate of individual molecules would be many orders of magnitude faster than that of particles, but the required concentration of dissolved molecules in the



**Figure 10** Volume-average diameter  $d_v$  of LDPE/PS 70/30 blends containing different amounts of S-E as the function of the annealing time in log-log scale



**Figure 11**  $G'$ ,  $G''$  and  $\eta'$  versus frequency  $\omega$  for PS and LDPE at 180°C

(incompatible) matrix to account for the kinetics of particle growth appears to be much too high for this process to occur. The problems associated with the kinetics of particle contact are discussed further in Appendix A. Jang *et al.*<sup>28</sup> used a movie camera to follow particle coalescence and noted that small particles (smaller than 5  $\mu\text{m}$ ) would wander about randomly, but more often the particles preferentially translated in a particular direction. They suggested that gravitational forces and possible local temperature gradients might play a role. However, there is no experimental evidence to support their suggestion and the mechanism remains to be explored.

Figure 7 shows SEM micrographs of the fracture surfaces of a blend containing 1% S-E which was annealed at 200°C for 0 and 5 min. It is seen that the addition of the S-E not only significantly decreased the sizes of the dispersed PS particles but also essentially prevented coalescence. With 1% added S-E, the dispersed PS particles had a  $d_v$  of 0.81  $\mu\text{m}$  before annealing and a  $d_v$  of only 0.89  $\mu\text{m}$  after annealing. The PS particle size distributions of the samples before and after annealing are shown in Figure 8. The

distribution was narrower for the sample with the block copolymer, and it did not change much upon annealing.

Figure 9 shows the  $d_v$  of the PS phases as a function of annealing time for LDPE/PS 70/30 blends containing different amounts of S-E. The sample without S-E shows a sharp increase in  $d_v$  during the first 30 min and then a more gradual increase with additional annealing time. The PS phase size of the blend with 0.25% S-E is very much smaller compared to the sample without S-E, i.e., 2 and 5.5  $\mu\text{m}$ , respectively, and the phase size increases only slightly with annealing time. It also shows that most of the change took place initially, with a much slower increase at later times. When more S-E is added to the blend, a further decrease in coalescence rate is observed, and with 1 and 3% S-E, the coalescence of the dispersed PS phase in these blends has been essentially suppressed.

Coalescence data for the above blends are replotted on a log  $d_v$ -log time basis in Figure 10. A linear relationship between log  $d_v$  and log annealing time is found for all samples, and the slopes of these linear curves represent coalescence rates. The slope for the blend containing 0.25% S-E is significantly lower than that of the uncompatibilized blend, i.e., 0.015 versus 0.023, respectively. With 1 and 3% S-E, the slopes are further decreased to 0.012. The rapid decrease of the coalescence rate with the addition of 0.25% S-E, followed by a more gradual change when more S-E is added, is quite similar to what is found for the dispersed phase size versus S-E concentration as shown in Figure 4. Since the phase size is proportional to the interfacial tension<sup>44</sup>, we find that the phase size and the coalescence rate decrease with the addition of S-E in a similar manner. However, the interfacial tension also correlates with the addition of block copolymer, so it is not clear whether the decrease in coalescence rate is governed by interfacial tension effects or from steric interaction effects associated with the block copolymer molecules in the interface, i.e., steric stabilization. Sundararaj and Macosko<sup>26</sup> suggested that surfaces of dispersed particles in a compatibilized blend are covered with thin layers of copolymers, with each block of the copolymer penetrating into the phases where it is miscible. When two such particles approach one another, the segments of copolymers on the surface of each particle do not allow the inner parts of two particles (the dispersed phase of the blend) to contact, and hence 'sintering' of the two particles cannot take place. The prevention of coalescence, we believe, however, is more likely due to the steric repulsion experienced by the block corona chains as a neighboring impenetrable particle approaches, i.e., the repulsion is due to the loss of configurational entropy<sup>45,46</sup> of the corona chains by the spatial constraints they experience when a neighboring particle comes within the span of the corona chains. The repulsive energy per corona chain can be quite large, i.e., 5–10 kT per chain when the interparticle spacing is reduced to one-half the *rms* end-to-end distance of the free chain.

To prevent particle coalescence, the surface coverage of the particle by copolymer does not have to be saturated, and that only the amount which can provide enough steric interactions is required. Macosko<sup>47</sup> has discussed the critical surface coverage required to prevent dynamic and static coalescence. Dynamic coalescence takes place during the melt blending and static coalescence takes place during annealing. Macosko reported that 0.01 chains/nm<sup>2</sup> are required for the prevention of dynamic coalescence and 0.03 chains/nm<sup>2</sup> are required for the prevention of static coalescence. Table 2 shows that the surface coverage for the

system containing 0.25% S-E is 0.023 chains/nm<sup>2</sup> which is slightly below the critical value of 0.03 chains/nm<sup>2</sup> given by Macosko and hence slightly unstable morphology would be predicted. This is in agreement with our experimental results. The values for 1 and 3% S-E are 0.037 and 0.064 chains/nm<sup>2</sup>, respectively, which are well above the critical value and hence stable morphologies are predicted, in agreement with our experimental results in Figure 9 showing that the coalescence processes in these two blends have practically stopped.

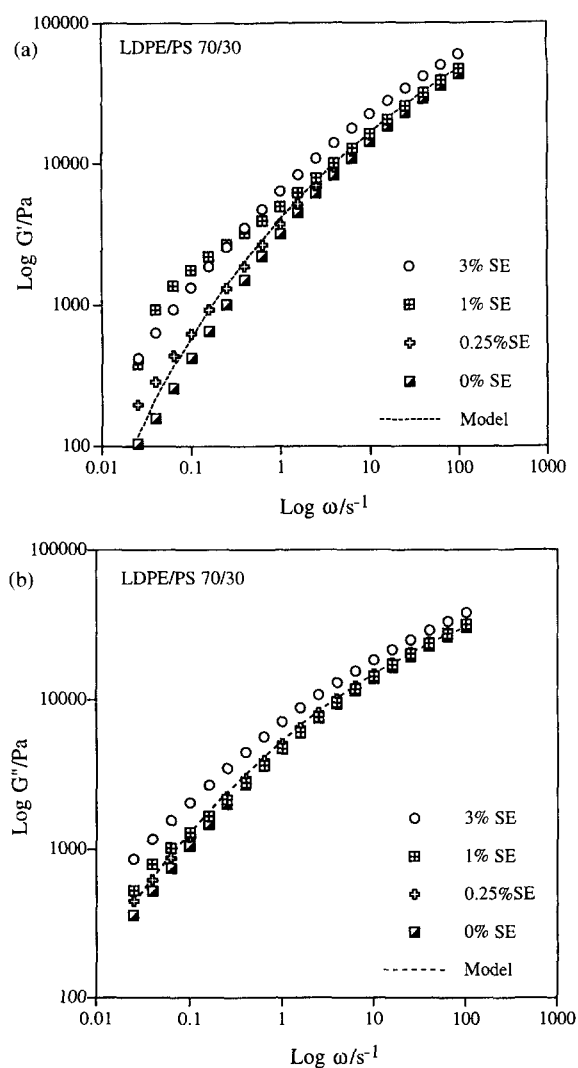
#### Rheological behavior

Figure 11 shows  $G'$ ,  $G''$  and  $\eta'$  as a function of frequency for PS and LDPE. PS has a higher molecular weight than LDPE and shows a higher dynamic viscosity. The frequency dependence of the dynamic moduli of LDPE/PS 70/30 blends containing different amounts of S-E are shown in Figure 12A and Figure 12B. The presence of the S-E block copolymer increases both the storage ( $G'$ ) and loss ( $G''$ ) moduli of the blends. The increase of  $G'$  in the low frequency region is in accordance with literature data<sup>37,38</sup>. Figure 13 shows the frequency dependence of the dynamic viscosity for the different blends, and shows that both the dynamic viscosity and non-Newtonian behavior increase with higher S-E concentrations.

The above effects of the S-E can be attributed to a combination of two factors: (1) the morphology change of the blend due to the addition of the S-E copolymer and, (2) the rheological properties of the S-E copolymer itself. We believe the dominant factor is that associated with the blend morphology. Figure 4 shows that the PS phase sizes are significantly smaller with the addition of the S-E, which results in a smaller distance between particles with a greater likelihood of particle-particle interaction. In addition, the effective distance between particles is also smaller because the span of the corona chains of the copolymer increases the effective size of a particle. We believe that these stronger inter-particle interactions are responsible for the increase in the dynamic properties as well as for the significant increase in viscosity of the blends when S-E is added. On the other hand, Brahim *et al.*<sup>41</sup> have suggested that the viscosity of the system is increased by the increased adhesion between the particles and the matrix provided by the block copolymer in the interface region. However, the mechanism by which this would occur is not clear.

When the concentration of copolymer is high, and beyond that required to saturate the interface, the remaining block copolymer can form micelles or a separate phase. Micelle formation can occur in both phases or in only one phase, depending on the molecular architecture of the block copolymer. In general, micelles will form preferentially in the phase which corresponds to the larger block of a diblock copolymer. For the blend with 3% S-E, we expect that micelles will form with equal probability in either phase since the blocks of the S-E block copolymer are essentially of equal size.

We have used a model by Palierne<sup>48</sup> and the calculation procedure by Bousmina *et al.*<sup>39</sup> to predict rheological properties of a blend from the rheological properties of the components of the blend. The Palierne model is an emulsion-type model which gives the rheological behavior of a dispersion of incompressible spherical viscoelastic inclusions in an incompressible viscoelastic matrix. It takes into account the polydispersity of particle sizes as well as the hydrodynamic interactions between particles. A basic assumption of the model is that the particle deformation is



**Figure 12** Dynamic moduli for blends with different concentration of S-E block copolymer: (A)  $G'$ ; (B)  $G''$ . The dotted line shows the predicted values of  $G'$  and  $G''$  from the Palierne model<sup>48</sup> for the blend without added S-E copolymer

small. The calculation of  $G'$  and  $G''$  of the blend requires knowledge of the morphology, the interfacial tension, and  $G'$  and  $G''$  for both phases in the same frequency range. We have used the experimental  $G'$  and  $G''$  data for PS and LDPE shown in Figure 11, and taken the interfacial tension between PS and PE at 180°C as 4.9 mN/M<sup>49</sup>. Since Bousmina *et al.*<sup>39</sup> have shown good agreement between the predicted and experimental values by using a volume-average radius and the total volume fraction of the dispersed phase, we have done the same and have taken the volume-average radius as 0.35  $\mu\text{m}$  (from Figure 4) and a volume fraction of the dispersed phase of 27%.

Model predictions for  $G'$  and  $G''$  and their comparison with the experimental data for the blend without S-E are shown in Figure 12A and Figure 12B. The predicted values of  $G'$  and  $G''$  are slightly higher than those found experimentally. The SEM micrographs in Figure 14 show the blend morphologies before and after the rheological measurements, and clearly show that the PS particles of the blend have been substantially elongated during the rheological measurements. Since the Palierne model<sup>48</sup> assumes small deformations of spherical particles, the lack of a quantitative fit between theory and experiment may be due to particle deformations that are larger than the theory allows.



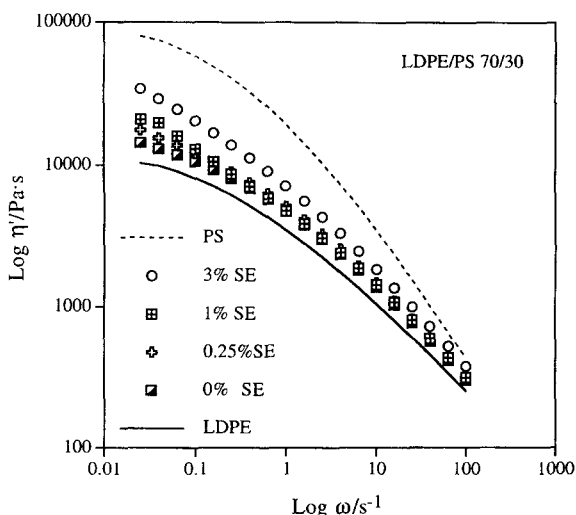


**Figure 13** Dynamic viscosity  $\eta'$  versus frequency for LDPE/PS blends with different concentrations of S-E copolymer

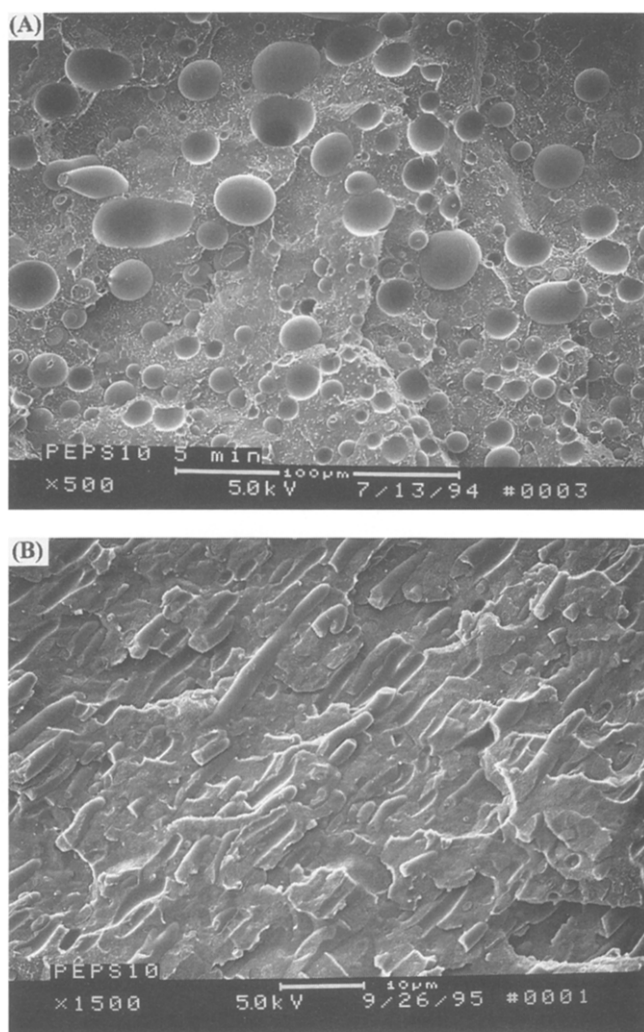


**Figure 14** SEM micrographs of fracture surfaces of LDPE/PS 70/30 blend: (A) before and (B) after rheological measurements

## CONCLUSIONS

Although the diblock copolymer usually shows a higher efficiency in reducing the phase size of a blend than does a triblock copolymer, the latter may be more efficient in improving the mechanical properties of the blend. Our

results suggest that interfacial activity (in terms of reducing the phase size) is a necessary but not a sufficient requirement for a compatibilizer to improve mechanical properties. An effective compatibilizer needs to be interfacially active to decrease phase sizes, but it must also improve the interfacial adhesion of the blend components by efficiently entangling with them in the interface. It appears that this occurs more efficiently with triblock than with diblock copolymers.

The coalescence rate of the dispersed phase in polymer blend during annealing can be very fast, especially in the early stages of annealing. However, our results show that a suitable block copolymer can significantly decrease the coalescence rate or even effectively suppress it, and hence stabilize the morphology of the blend. The retardation of the coalescence by the block copolymer can be attributed both to the smaller interfacial tension between the blend components, and to steric interactions of the copolymer chains at the interface. It is difficult to separate these effects since the reduction in interfacial tension is directly related to the concentration of block copolymer in the interface, as is the steric stabilization properties of the copolymer.

The rheological properties of LDPE/PS blends compatibilized with a PE-*b*-PS block copolymer depend on the block copolymer concentration. The addition of the copolymer results in increases of the elastic modulus  $G'$  and the dynamic viscosity  $\eta'$  of the blend (particularly in the low frequency region), and the viscosity becomes more non-Newtonian. We attribute these effects to stronger particle-particle interactions due to the smaller particle sizes when the interfacially active block copolymer is present, and to the steric interaction of the corona chains of the block copolymers in the interface.

The Palierne model has been used to predict  $G'$  and  $G''$  of the blend without added block copolymer, and the predicted results agree qualitatively with the experimental results. The lack of quantitative agreement may be attributed to the observed large deformation of the particles during the rheological measurements.

## ACKNOWLEDGEMENTS

This work was supported by the National Institute of Standards and Technology under a Department of Commerce Advanced Technology Project grant. We thank Mr. Kevin Battjes for his help with SEM, and Ms. Katherine Robertson for her help in photography. Authors are very grateful to Dr. N. Seung for his synthesis of the S-E-S block copolymer.

## APPENDIX A:

In this section, we attempt to establish order-of-magnitude estimates of the kinetics of inter-particle contacts, in which estimates will be based on three possible mechanisms: (1) diffusional transport of spherical particles by Brownian motion, (2) attraction between particles from Van der Waals forces and, (3) dissolution and diffusion of individual polymer molecules. The results will be compared with the experimental findings in which the volume-average particle diameter increased from 5.5 to 7.3  $\mu\text{m}$  in 5 min at 200°C. This increase in size requires that a particle must coalesce with an average of 2.3 other particles (of equal size) in the 5-min period.

### A1. Diffusion of spherical particles

The diffusion coefficient of spherical particles  $D$  can be estimated from the Stokes–Einstein equation  $D = kT/6\pi\eta r$ , where  $k$  is the Boltzmann's constant ( $1.38 \times 10^{-23}$  J molecule $^{-1}$  K $^{-1}$ ),  $T$  is the temperature,  $\eta$  is the viscosity of the matrix, and  $r$  is the particle radius. For our system with  $\eta = 3 \times 10^4$  poise,  $r = 2.75 \mu\text{m}$  and  $T = 473$  K,  $D$  becomes  $4 \times 10^{-16}$  cm $^2$ /s =  $4 \times 10^{-8}$   $\mu\text{m}^2$ /s. Assuming that the particles are of equal size and are spaced equally apart, the distance  $d$  between particle centers is  $d = 1.8r/\phi^{1/3}$ , where  $\phi$  is the volume fraction of the dispersed phase. With  $\phi = 0.27$  and  $r = 2.75 \mu\text{m}$ ,  $d$  becomes  $2.78 \mu\text{m}$ , and the distance  $h$  between particles ( $h = d - 2r$ ) is  $h = 0.78 \mu\text{m}$ . The time  $t$  required for Brownian motion to bring two particles together which are separated by a distance  $h$  can be estimated from  $t = h^2/2D$ . Thus for the present system with  $h = 0.78 \mu\text{m}$  and  $D = 4 \times 10^{-8}$   $\mu\text{m}^2$ /s, the time required becomes  $7.6 \times 10^6$  s, which is approximately 25 000 times longer than the experimental time scale. Thus it seems unlikely that particle contact is the direct result of Brownian motion. Of course, the actual distribution of particles in space will not be uniform as assumed. Some particles will be closer together than the average assumed, but then others will be farther apart, thus more-or-less canceling out the influence of spacing. The diffusion rate would also be faster for smaller particles in the system and their average spacing would also be less, thus presumably acting to increase the coalescence rate. However, the number of smaller particles needed to coalesce with larger particles to increase the particle size by the amount observed would also increase. The diffusion rate  $D \sim 1/r$  and the diffusion distance  $d \sim r$ , thus the diffusion time  $t \sim d^2/D \sim r^3$ . However, the number of coalescing particles required to increase the size of a given particle is proportional to  $1/r^3$ , thus there is a balance between the time scale for diffusion and the number of particles that must coalesce. Hence it seems unlikely that a distribution of particle sizes is responsible for the very large difference between the calculated and observed coalescence kinetics.

### A2. Particle migration driven by Van der Waals attractive forces between particles

The Van der Waals force  $F_v$  between two spherical particles of equal size can be estimated<sup>50</sup> as  $F_v = Ar/12h^2$ , where  $A$  is the Hamaker constant, and  $r$  and  $h$  are the particle radius and separation, respectively. The Hamaker constant for particles in vacuum is typically<sup>50</sup>  $A \sim 10^{-19}$  J. For particles imbedded in a resin matrix, the Hamaker constant would be very much less, but for the purposes of establishing what the maximum interaction force might be, we shall use this value of  $A = 10^{-19}$  J. The attractive force then becomes  $F_v = 3.8 \times 10^{-14}$  N for our system with  $r = 2.75 \mu\text{m}$  and  $h = 0.78 \mu\text{m}$ . The particle migration velocity  $v$  can then be obtained by equating the attractive Van der Waals force  $F_v$  and the frictional force  $F_s$  from the Stokes equation  $F_s = 6\pi\eta r v$ , where  $v$  is the particle velocity. This gives  $v = 2.7 \times 10^{-7}$   $\mu\text{m}$ /s. Thus the time required for two particles each to migrate  $0.39 \mu\text{m}$  to come together would be  $1.4 \times 10^6$  s, again very much longer than the observed experimental time scale for coalescence. Of course, the attractive force would increase as the particles came closer together (as  $1/h^2$ ) which would decrease the calculated time somewhat, but the (vacuum) value of the Hamaker constant  $A$  used here is undoubtedly very much larger than the true value for

particles imbedded in a matrix, so this calculated time is undoubtedly a minimum value.

### A3. Dissolution and migration of individual molecules

In this model, we assume that polymer molecules from the smaller dispersed particles dissolve in the matrix phase and then diffuse to the larger particles (which have a lower chemical potential  $\mu_p \sim 1/r$ ). The diffusion rate of individual molecules will be much faster than that of the particles themselves, but the actual value for any particular system is in question. We shall assume that  $D = 10^{-10}$  cm $^2$ /s =  $10^{-2}$   $\mu\text{m}^2$ /s for purposes of this order-of-magnitude calculation. The time required for a molecule to diffuse  $1 \mu\text{m}$  (taken as an average spacing between particles where  $r \sim 3 \mu\text{m}$  and  $\phi \sim 0.25$ ) would then be 100 s. The observed increase in size of the dispersed particles from  $r = 2.75 \mu\text{m}$  to  $r = 3.65 \mu\text{m}$  corresponds to the addition of  $3.5 \times 10^7$  molecules to a particle, taking the molecular weight  $M$  as 160 000. Experimentally, the time required for the increase in size was 300 s, which is three times longer than the average diffusion time. So the average number  $n$  of molecules in the space between particles at any given time would be  $n \cong 1/3(3.5 \times 10^7) \cong 12 \times 10^6$ . The volume concentration  $\phi$  of the polymer in this space would then be  $\phi = (12 \times 10^6 M/N_A)/\{4\pi(r'^3 - r^3)/3\}$ , where  $N_A$  is Avogadro's number. Taking  $r = 3 \mu\text{m}$  and  $r' - r = 1 \mu\text{m}$ , the volume fraction of dissolved polymer in the space between particles becomes 0.021. This is an unrealistically high concentration for two polymers that are as immiscible as are polyethylene and polystyrene. Simple calculations using Flory-Huggins theory would place the solubility of polystyrene in polyethylene many orders-of-magnitude lower than the calculated value, i.e.,  $\phi \sim \exp(-N_{\text{PS}}\chi)$ , where  $N_{\text{PS}}$  is the number of PS segments and  $\chi$  is the Flory interaction parameter per segment. The actual value of  $\chi$  for the PS/PE pair is not known, but must be larger than that for polystyrene/polyisoprene, for which  $\chi$  is reported<sup>51</sup> to be  $6.5 \times 10^{-2}$  per monomer unit. Using this value as a minimum,  $\phi$  is predicted to be  $< 10^{-43}$  for polystyrene with  $M_n = 160\,000$ . Of course, this is an unrealistic number, but it does indicate that the actual solubility of the polystyrene of 160 000 molecular weight in PE will be vanishingly small. Even if the diffusion constant of PS in the polyethylene matrix is much larger than the assumed value of  $10^{-10}$  cm $^2$ /s and the diffusion distance is much smaller, there are no realistic values that would allow for the observed coalescence kinetics by this molecular diffusion process, given the extreme immiscibility of PE and PS.

In conclusion, all three of the kinetic processes considered here for coalescence present problems, in that none even comes close to rationalizing the observed kinetics. All three processes have time scales that are vastly longer than the experimental time scale. The actual mechanism that brings particles together at the rate observed remains an enigma.

## REFERENCES

1. Paul, D. R., in *Polymer Blends*, Vol. 2, Chap. 12, ed. D. R. Paul and S. Newman. Academic Press, New York, 1978.
2. Fayt, R., Jerome, R. and Teyssie, Ph., in *Multiphase Polymers: Blends and Ionomers*, Chap. 2, ed. L. A. Utracki and R. A. Weiss. ACS, Washington, DC, 1989.
3. Locke, C. E. and Paul, D. R., *J. Appl. Polym. Sci.*, 1973, **17**, 2719.
4. Heikens, D., Hoen, N., Barentsen, W., Peit, P. and Ladan, H., *J. Polym. Sci. Polym. Symp.*, 1978, **62**, 309.

5. Fayt, R., Jerome, R. and Teyssie, Ph., *J. Polym. Sci. Polym. Lett. Edn.*, 1981, **19**, 79.
6. Fayt, R., Jerome, R. and Teyssie, Ph., *J. Polym. Sci. Polym. Phys. Edn.*, 1981, **19**, 1269.
7. Fayt, R., Jerome, R. and Teyssie, Ph., *J. Polym. Sci. Polym. Lett. Edn.*, 1988, **26**, 2209.
8. Fayt, R., Jerome, R. and Teyssie, Ph., *Makromol. Chem.*, 1986, **187**, 837.
9. Fayt, R., Jerome, R. and Teyssie, Ph., *J. Polym. Sci. Polym. Lett. Edn.*, 1986, **24**, 25.
10. Fayt, R., Jerome, R. and Teyssie, Ph., *J. Polym. Sci. Polym. Lett. Edn.*, 1989, **27**, 481.
11. Patterson, H. T., Hu, K. H. and Crindstaff, T. H., *J. Polym. Sci. Polym. Symp.*, 1971, **34**, 31.
12. Gailard, P., Ossenbach-Sauter, M. and Riess, G., *Makromol. Chem. Rapid Commun.*, 1980, **1**, 771.
13. Gailard, P., Ossenbach-Sauter, M. and Riess, G., in *Polymer Compatibility and Incompatibility: Principles and Practice*, ed. K. Solc. MMI Symposium Series 2, Harwood, New York, 1982.
14. Anastasiadis, S. H., Gancarz, I. and Koberstein, J. T., *Macromolecules*, 1989, **22**, 1449.
15. Elemans, P. H. M., Janssen, J. M. H. and Meijer, H. E., *J. Rheol.*, 1990, **34**, 131.
16. Wagner, M. and Wolf, B. A., *Polymer*, 1993, **34**, 1460.
17. Leibler, L., *Makromol. Chem. Macromol. Symp.*, 1988, **16**, 1.
18. Noolandi, J. and Hong, K. M., *Macromolecules*, 1982, **15**, 482.
19. Noolandi, J. and Hong, K. M., *Macromolecules*, 1984, **17**, 1531.
20. Noolandi, J., *Polym. Eng. Sci.*, 1984, **24**, 70.
21. Lindsey, C. R., Paul, D. R. and Barlow, J. W., *J. Appl. Polym. Sci.*, 1981, **26**, 1.
22. Paul, D. R., in *Thermoplastic Elastomers*, Chap. 12, Section 6, ed. N. R. Legge, G. Holden and H. E. Schroeder. Hanser, Munich, 1987.
23. Kim, K. U. and Meier, D. J., *Polymer (Korea)*, 1989, **13**, 40.
24. Periard, J. and Riess, G., *Colloid Polym. Sci.*, 1975, **253**, 362.
25. Thomas, S. and Prud'homme, R.E., *Polymer*, 1992, **33**, 4260.
26. Sundararaj, U. and Macosko, C. W., *Macromolecules*, 1995, **28**, 2647.
27. McMaster, L. P., *Adv. Chem. Ser.*, 1975, **142**, 43.
28. Jang, B. Z., Uhlmann, D. R. and Vander-Sande, J. B., *Rubber Chem. Technol.*, 1984, **57**, 291.
29. Favis, B. D., *J. Appl. Polym. Sci.*, 1990, **39**, 285.
30. Fortenly, I. and Kovar, J., *Polym. Compos.*, 1988, **9**, 119.
31. Datta, S. and Lohse, D. J., *Macromolecules*, 1993, **26**, 2064.
32. Endo, S., Min, K., White, J. L. and Quirk, R. P., *Polym. Eng. Sci.*, 1986, **26**, 45.
33. Nakayama, A., Guegan, P., Hirao, A., Inoue, T. and Macosko, C. W., *Polym. Prepr.*, 1993, **34**(2), 820.
34. Guegan, P., Macosko, C. W., Ishizone, T., Hirao, A. and Nakahama, S., *Macromolecules*, 1994, **27**, 4993.
35. Leibler, L., *Macromolecules*, 1982, **15**, 1283.
36. Utracki, L. A. and Sammut, P., *Polym. Eng. Sci.*, 1988, **28**, 1405.
37. Haaga, S. and Friedrich, C., *Polym. Networks Blends*, 1994, **4**, 61.
38. Riemann, R.-E., Braun, H., Weese, J. and Schneider, H. A., *Polym. Prepr.*, 1993, **34**(2), 801.
39. Bousmina, M., Pataille, P., Sapeiha, S. and Schreiber, H.P., *J. Rheol.*, 1995, **39**, 499.
40. Kim, K. U. and Meier, D. J., *Polymer (Korea)*, 1989, **13**, 119.
41. Brahim, B., Ait-Kadi, A., Ajji, A., Jerome, R. and Fayt, R., *J. Rheol.*, 1991, **35**, 1069.
42. Taylor, G. I., *Proc. R. Soc. London*, 1932, **A138**, 41.
43. Taylor, G. I., *Proc. R. Soc. London*, 1934, **A146**, 501.
44. Wu, S., *Polym. Eng. Sci.*, 1987, **27**, 335.
45. Meier, D. J., *J. Phys. Chem.*, 1967, **71**, 1861.
46. Napper, D. H., *Polymeric Stabilization of Colloidal Dispersions*. Academic Press, New York, 1983.
47. Macosko, C. W., in *Compatibilization of Polymer Blends*. Turner Alfrey Visiting Professor Course, Midland, MI, 1995.
48. Paliarne, J. F., *Rheol. Acta*, 1990, **29**, 204.
49. Brandrup, J. and Immergut, E. H., *Polymer Handbook*, 3rd edn. Wiley Interscience, New York, 1989, p. VII427.
50. Israelachvili, J., *Intermolecular and Surface Forces*, 2nd Ed., Academic Press, London, 1992, p. 178.
51. Rounds, N. A., Doctoral Dissertation, University of Akron, 1970.